

GEODESIC SHOOTING FOR COMPUTATIONAL ANATOMY

MICHAEL I. MILLER, ALAIN TROUVÉ, AND LAURENT YOUNES

ABSTRACT. Studying large deformations with a Riemannian point of view has been an efficient point of view to generate metrics between deformable objects, and to provide accurate, non ambiguous and smooth matchings between images.. In this paper, we study the geodesic of such large deformation diffeomorphisms, and more precisely, introduce an fundamental property that they satisfied, namely the conservation of momentum. This property allows to generate and store complex deformations with the help of one initial “momentum” which serves as the initial state of a differential equation in the group of diffeomorphisms. Moreover, it is shown that this momentum can be also used for describing a deformation of a given visual structure, like points, contours or images, and that, in this case, it has the same dimension, as a consequence of the normal momentum constraint we introduce.

1. INTRODUCTION

Over the past several years our group has been studying natural shapes using homogeneous orbits of imagery constructed via the action of transformation groups on exemplars or templates. The mathematical structure of group action as a model in image analysis has been pioneered by Grenander [11], the idea being to introduce the group actions in the very nature of the objects themselves, through the notion of *deformable templates*. Roughly speaking, a deformable template simply is an “object or exemplar” I_{temp} on which a group G acts and generates, through the orbit $J = G.I_{\text{temp}}$, a whole family of new objects. The interest of this approach is to concentrate the modeling effort on the group G , and not on the family of objects J .

Since the earliest introduction by Silicon Graphics Incorporated of special purpose graphics hardware for object rendering, group action as a model in image analysis has been the subject of a wide range of research in computer vision. Naturally, the analytical and computational properties of the low-dimensional matrix Lie groups form the core dogma of modern Computer graphics. In sharp contrast, however, for the study of imagery generated from natural or Biological shapes, the finite dimensional matrix groups are replaced by their infinite dimensional analogue, the more general diffeomorphisms [5, 34, 9, 14, 21, 20]. Diffeomorphisms $\phi \in G$ defined on the background

space $\Omega \subset \mathbb{R}^d$ are generated as flows of the equations

$$\frac{d\phi_t}{dt} = v_t \circ \phi_t, \quad \phi_0 = \text{id}, t \in [0, 1]. \quad (1)$$

This is the principal focus in Computational Anatomy, the study of shape via high dimensional transformation generated via the flows of Eqn. (1). In this setting, the matrix groups oftentimes play a subordinate or nonprimary role as nuisance variables.

The anatomical orbit or deformable template is made into a metric space with a metric distance between elements by constructing curves through the space of diffeomorphisms connecting them; the length of the curve becomes the basis for the construction, the metric distance corresponding to the geodesic shortest length curves. This gives rise to a natural variational problem describing the geodesic flows between elements in the orbit, with the solution of the associated Euler-Lagrange equations giving the optimal flow of diffeomorphisms and thus the metric between the shapes. The obtained setting shares several similarities with the mechanics of perfect fluids, for which the Euler-Lagrange equation has been derived by Arnold (Equation 1 of [2]) for the group of divergence-free volume-preserving diffeomorphisms. As well these results become another example of the general Euler-Poincaré principle of [17] but applied to the infinite dimensional setting.

Interestingly, as emphasized by Arnold [1] in his study, one of the most beautiful aspects of studying diffeomorphisms with a Lie group point of view is that many fundamental aspects which can be proved in the finite dimensional case can be formally extended to retrieve well-known equations of mechanics. One of the purposes of this paper is to develop infinite dimensional analogues for the study of high dimensional shapes via diffeomorphisms, of several of the well known properties of Lie groups in rigid body mechanics. In particular we shall focus on the interpretation of the Euler equation as an expression of the evolution of the generalized momentum of the diffeomorphic flow $\phi_t, t \in [0, 1]$ in both Eulerian and Lagrangian coordinates.

Such a point of view will link our geodesic formulation to a *conservation of momentum law* in Lagrangian coordinates providing a powerful method for studying and modeling diffeomorphic evolution of shape. It will imply that the momentum of the diffeomorphic flow at any place along

the geodesic can be generated from the momentum at the origin, thus providing the vehicle for *geodesic generation via shooting*.

This same conservation of momentum of the diffeomorphic flow, allows us to derive equations for the geodesic evolution of the elements in the orbit $I_t = I \circ \phi_t, t \in [0, 1], I \in \mathcal{J}$. This unifies various geodesic evolutions associated with orbits of sparse finite dimensional landmarked shapes as well as the evolutions of dense images arising. Of special interest is the fact that for the special case of image matching, geodesic evolution of elements in the orbit links us to the notion of normal motion familiar to the rapidly growing community working in *level set methods*. Interestingly, as we show, the momentum of the diffeomorphic flow is normal to the level sets associated with geodesic motion. By solving the partial differential equations which are associated with the conservation of momentum, we will be able to control, by specifying the initial conditions (within a specific class of momentum which depends on the considered imaging problem) a wide range of arbitrarily large deformations; this provides new possibilities for learning shape models of deformable templates, or for designing new numerical matching procedures.

This second point of view in terms of the conservation of momentum law also sheds new light on a large number of high dimensional evolution based Active Model Methods in Computer Vision, including active snakes and contours [16, 29, 39, 35, 27, 10, 36, 4, 38, 18, 41], active surfaces and deformable models [31, 19, 6, 7, 30, 22, 40, 37, 26, 38, 23, 28]. In such approaches vector fields are defined which give the boundary manifold of the shape some velocity of motion, usually following the gradient of an energy to form an attractive force to pull the boundary. The power of such methods is that they parameterize motion only associated with a submanifold of the imagery, not the entire extrinsic background space. For example, to deform a planar simply connected shape via an active contour method, the dimension of the motion is determined by the dimension of the boundary of the region, which is substantially less than the dimension of the plane. Historically such approaches have not been studied globally as diffeomorphic action. In fact it is well known that such methods cannot prevent self intersection nor ensure topological consistency, for which the addition of other constraints become necessary [12, 13]. From the conservation law in Lagrangian

coordinates describing geodesic motion in the metric space of diffeomorphic action, we introduce the *normal momentum motion* which constrains the momentum to the bounding manifold, and extends the velocity of motion of the shape to the entire background space, thereby giving the global property that the resulting integrated vector field generates a diffeomorphism on the entire extrinsic space. This in turn carries the smooth submanifold diffeomorphically. As the analysis shows, this global property seems to be required to generate consistent motions.

2. THE BASIC SET UP

2.1. Right invariant metric on group of diffeomorphisms. We briefly recall the construction underlying the groups of diffeomorphisms we consider. Fix an open, bounded subset $\Omega \subset \mathbb{R}^d$. Following [33], the construction is based on the design of a “Lie algebra” \mathfrak{g} (we will see below that it is not really a Lie algebra, but still retain the term), which is in turn used to generate the group elements. The elements of \mathfrak{g} , as instantaneous variations of diffeomorphisms, can be identified to vector fields on Ω . The following construction of \mathfrak{g} will be assumed. We denote by H the set of square integrable vector fields on Ω with the usual L^2 metric, and consider an operator $L : v \mapsto Lv \in H^* = H$ which is assumed to be defined on a domain $D(L)$ containing all smooth (C^∞) vector fields with compact support in Ω . This operator induces an inner product on $D(L)$ by $\langle v, w \rangle_L = (Lv, w)$. Under some condition, namely that L is symmetric and strongly monotone ([42]), this prehilbertian structure can be completed to form a Hilbert space, denoted \mathfrak{g}_L which is continuously embedded in H (Freidrich’s extension). Under this extension, L can be seen as an isometry between \mathfrak{g}_L and \mathfrak{g}_L^* . When \mathfrak{g}_L can be, in addition, embedded into $C^p(\Omega)$, the set of p times continuously differentiable vector fields on Ω , with $p \geq 1$ (which means that, for some constant K and for all smooth v , $(Lv, v) \geq K \|v\|_{p,\infty}$, with $\|v\|_{p,\infty}$ being the supremum norm of v and its derivatives up to p -th order over Ω), then, the following can be shown ([33, 9]): if $t \mapsto v_t$ is a time-dependent family of elements of \mathfrak{g}_L such that $\int_0^1 \|v_t\|_L dt < \infty$, ie $v \in L^1([0, 1], \mathfrak{g}_L)$, then the ODE $\frac{d\phi_t}{dt} = v_t \circ \phi_t$ with initial conditions $\phi_0(x) = x, x \in \Omega$, can be integrated over $[0, 1]$, and ϕ_1 is a diffeomorphism of Ω , which is denoted ϕ_1^v . The image of $L^1([0, 1], \mathfrak{g}_L)$ by $v \mapsto \phi_1^v$ forms

our group of diffeomorphisms (which is therefore specified by the operator L) denoted $G = G_L$ (we shall also set $\mathfrak{g} = \mathfrak{g}_L$ in the following, since the operator L will be fixed).

We shall only consider paths $\phi : [0, 1] \rightarrow G$ defined by $\frac{d\phi}{dt} = v_t(\phi_t)$ for which the kinetic energy, given by, $E(\phi) = \int_0^1 (Lv_t, v_t) dt$ where $v : [0, 1] \rightarrow \mathfrak{g}$, is finite. Moreover, we shall use the notation $\phi_t^v(x)$ for the solution at time t of $dy/dt = v_t(y)$ with initial condition $y(0) = x$, and also denote

$$\phi_{st}^v = \phi_t^v \circ (\phi_s^v)^{-1} \tag{2}$$

(so that $\phi_t^v = \phi_{0t}^v$ and $\phi_{t0}^v = (\phi_t^v)^{-1}$).

2.2. Lagrangian and Eulerian frames. Time dependent diffeomorphisms on Ω can be thought of as the motion of a fluid. To understand correctly the meaning of the conservation of momentum, and to motivate the Lie group formalism which is introduced below, it is important to be able to make a clear distinction between the so-called *Eulerian coordinates* and *Lagrangian coordinates* for the description of motion.

A time-dependent diffeomorphism is a function $\phi_t : \mathbb{R}^d \rightarrow \mathbb{R}^d$ which associates to each point x_0 at time 0 its position $x_t := \phi_t(x_0)$ at time t . The diffeomorphism ϕ_t makes the connection between two frames, the Lagrangian frame at time 0 and the Eulerian frame at time t . In the Eulerian frame, the velocities of particles of fluid are given by a vector field $v_t^e : \mathbb{R}^d \rightarrow \mathbb{R}^d$ such that $v_t^e(x_t)$ is the speed of a particule located at x_t at time t . Hence,

$$v_t^e(y) = \frac{d}{ds} (\phi_{t+s}(\phi_t^{-1}(y)))|_{s=0} \text{ i.e. } \frac{d\phi_t}{dt}(x_0) = v_t^e(\phi_t(x_0))$$

Pulling back v_t^e in the Lagrangian frame at time 0, we obtain a new vector field v_t^l , uniquely defined by

$$v_t^l(x) = \frac{d}{ds} (\phi_t^{-1}(\phi_{t+s}(x)))|_{s=0} \text{ i.e } v_t^l = (d\phi_t)^{-1}(v_t^e \circ \phi_t)$$

This pull back is more concretely characterized by the property: if $s \rightarrow \gamma_l(s)$ is a smooth curve such that $\gamma_l(0) = x_0$ and $\frac{d\gamma_l}{ds}|_{s=0} = v_t^l(\gamma_l(0))$ then $\gamma_e(s) \doteq \phi_t(\gamma_l(s))$ satisfies $\frac{d\gamma_e}{ds}|_{s=0} = v_t^e(\gamma_e(0))$.

The operation

$$v \mapsto (d\phi)v \circ \phi^{-1}$$

defines a fundamental Lie group operation, and is called the adjoint action of G on its Lie algebra (here composed of vector fields), denoted $\text{Ad}_\phi v$. We have obtained the relation

$$v_t^e = \text{Ad}_{\phi_t} v_t^l$$

To interpret the adjoint action pictorially, the new vector field under the adjoint action $v \rightarrow \hat{=} (d\phi)v \circ \phi^{-1}$ has to be interpreted as the transformation of v under the deformation generated by ϕ . Figure 1 shows how the field v^l at location x is transported by the flow to the value $v^e(y)$ at location $y = \phi(x)$ by pushing forward (using ϕ) the Lagrangian frame on which v^l is drawn. Note that the orientation of the vector $v^e(x)$ drawn on the deformed sheet is also changed (through the action of $(d\phi)$).

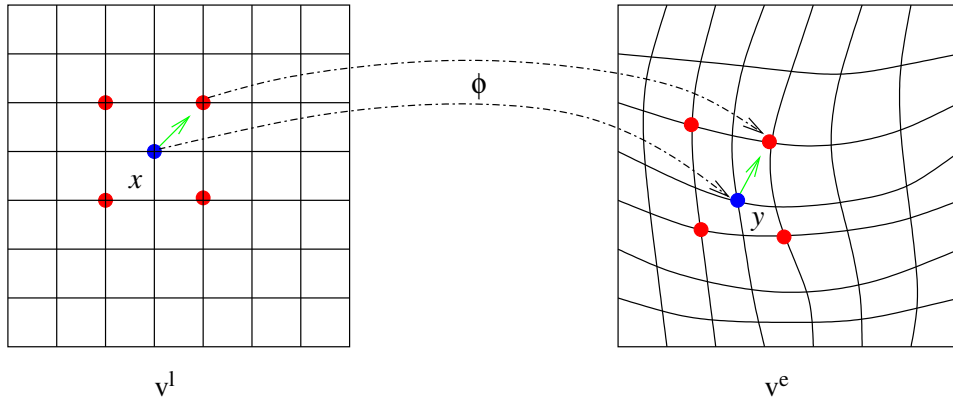


FIGURE 1. Here is represented the deformation obtained by pulling back the Eulerian frame associated with v^e and represents pictorially the adjoint action.

2.3. Momentum in Eulerian and Lagrangian coordinates. The momentum of the system at time t will be a continuous linear form M_t^e which is applied to the velocity v_t^e to yield the energy at time t : $W_t = (M_t^e, v_t^e)$. As a continuous linear form which can be applied to an element of \mathfrak{g} , M_t^e belongs to the dual space \mathfrak{g}^* . The key assumption which is made in this paper is that there exists an operator, denoted L , defined on \mathfrak{g} , with values in \mathfrak{g}^* such that $M_t^e = Lv_t^e$. This assumption first implies that there is no other contribution to the energy, except that which is provided by the motion; there is in particular no external force. The second consequence comes from the fact that L is constant with respect to time: the physical properties are the same whatever

deformation is applied. The physical analogy would be an incompressible perfect fluid, under the additional assumption $\operatorname{div} v_t^e = 0$ (we do not make such an assumption in this paper). Using Lie group terms, this corresponds to the fact that the energy of the fluid is computed by integrating a right-invariant metric along the deformation path. The operator L which is introduced here is the same as the operator used in section 2.1 for the construction of the group G .

The adjoint action can be used to derive the conservation law transferring from Eulerian to Lagrangian coordinates; denoting (Lv_t^e, v_t^e) the energy at time t , then

$$(Lv_t^e, v_t^e) = (Lv_t^e, Ad_{\phi_t} v_t^l) = (Ad_{\phi_t}^* Lv_t^e, v_t^l)$$

This leads to the definition $M_t^l = Ad_{\phi_t}^* M_t^e$ of the momentum in Lagrangian coordinates, which, as will be illustrated below, is constant over time along any energy minimizing path.

3. GEODESIC EVOLUTION OF THE DIFFEOMORPHISM AND CONSERVATION OF MOMENTUM

3.1. Euler Equation as Evolution Equation for the Momentum in Eulerian Coordinates. The derivation of the Euler equation for extremal paths of the kinetic energy in the case of finite-dimensional Lie groups with a right invariant metric can be carried out in full generality within the Lie theory framework, to lead to the law of conservation of momentum. A general computation can be found in [1]. In our infinite dimensional case, a rigorous derivation of this law is much harder, and must most of the time be obtained directly from variational and functional analysis arguments rather than with purely algebraic Lie group derivations. However, it is interesting, and quite informative, to use these derivations to obtain a formal proof of the conservation of momentum, without wondering too much about the well-posedness of the expressions. This will be done in the next paragraphs.

The first Euler equation provides the variations of the momentum in Eulerian coordinates. Before stating it, we need some definitions:

Definition 1. *The adjoint action Ad of G on \mathfrak{g} and the associated adjoint action ad of \mathfrak{g} on itself are given with their dual operators Ad^*, ad^* by*

$$Ad_\phi w = (d\phi)w \circ \phi^{-1}, \quad (Ad_\phi^* f, w) = (f, Ad_\phi w); \quad (3)$$

$$ad_v w = [v, w] = (dv)w - (dw)v, \quad (ad_v^* f, w) = (f, ad_v w). \quad (4)$$

with $\phi \in G, w \in \mathfrak{g}, f \in \mathfrak{g}^*$.

Already at this point, one can point out the difficulty of the infinite dimensional problem: if v, w belong to \mathfrak{g} , it cannot be guaranteed that it is still so for $[w, v] = (dw)v - (dv)w$: in situations of interest, \mathfrak{g} is, in fact, not a Lie algebra: $Ad_\phi w$ and $ad_v w$ do not necessarily belong to \mathfrak{g} . As a consequence, the definition of $ad_v^* f$ which has been given cannot hold without some restriction on f , in order to be able to extend it to vector fields which are brackets of elements of \mathfrak{g} . We however proceed with such formal computation without addressing these issues. An interesting reading of these proofs may be done under the assumption that G is a group of linear transformations (and $\Omega = \mathbb{R}^d$), in which case the computations are trivially rigorous.

The geodesics are extremal curves for the kinetic energy. They satisfy an Euler equation giving the variation of the momentum in terms of the co-adjoint action operator on the momentum.

Statement 1. *The Euler equation for the kinetic energy is given by*

$$\frac{dLv}{dt} + ad_v^*(Lv) = 0. \quad (5)$$

When $Lv \in H$ (ie. it is a function), one has

$$ad_v^* Lv = \operatorname{div}(Lv \otimes v) + dv^* Lv. \quad (6)$$

where $\operatorname{div}(u \otimes v) = duv + \operatorname{div}(v)u$.

These equations, which are derived below, are special cases of the Euler-Poincaré principle, described, for example in [17].

Formal Justification. Consider a small variation $\phi_t \rightarrow \phi_t + \varepsilon \eta_t \circ \phi_t$. We want to identify the corresponding variation of v_t , ie. we want to identify h_t such that

$$\frac{d}{dt}(\phi_t + \varepsilon \eta_t \circ \phi_t) = (v_t + \varepsilon h_t + o(\varepsilon)) \circ (\phi_t + \varepsilon \eta_t \circ \phi_t)$$

Since this can be written,

$$\begin{aligned} \frac{d}{dt}(\phi_t + \varepsilon \eta_t \circ \phi_t) &= v_t \circ (\phi_t + \varepsilon \eta_t \circ \phi_t) + \varepsilon h_t \circ (\phi_t + \varepsilon \eta_t \circ \phi_t) + o(\varepsilon) \\ &= v_t \circ \phi_t + \varepsilon d_{\phi_t} v_t \eta_t \circ \phi_t + \varepsilon h_t \circ \phi_t + o(\varepsilon) \end{aligned}$$

and since

$$\begin{aligned} \frac{d}{dt}(\phi_t + \varepsilon \eta_t \circ \phi_t) &= \frac{d\phi_t}{dt} + \varepsilon \frac{d\eta_t}{dt} \circ \phi_t + \varepsilon d_{\phi_t} \eta_t \cdot \frac{d\phi_t}{dt} \\ &= v_t \circ \phi_t + \varepsilon \frac{d\eta_t}{dt} \circ \phi_t + \varepsilon d_{\phi_t} \eta_t v_t \circ \phi_t \end{aligned}$$

we have (applying ϕ_t^{-1} on the right to both terms)

$$h_t = \frac{d\eta_t}{dt} + d\eta_t v_t - dv_t \eta_t = \frac{d\eta_t}{dt} + [\eta_t, v_t].$$

Since¹

$$\int_0^1 \|v_t + \varepsilon h_t\|_L^2 dt \simeq \int_0^1 \|v_t\|_L^2 dt + 2\varepsilon \int_0^1 \langle v_t, h_t \rangle_L dt,$$

the first variation of the energy yields, for geodesic paths,

$$\int_0^1 \left\langle v_t, \frac{d\eta_t}{dt} + [\eta_t, v_t] \right\rangle_L dt = \int_0^1 (Lv_t, \frac{d\eta_t}{dt}) dt - \int_0^1 (Lv_t, ad_{v_t} \eta_t) dt = 0$$

which yields, after an integration by parts of the first integral

$$\int_0^1 \left(\frac{dLv_t}{dt}, \eta_t \right) dt + \int_0^1 (ad_{v_t}^* Lv_t, \eta_t) dt = 0$$

which provides the result since this is true for all paths η_t in \mathfrak{g} .

We now prove equation (6) under the assumption that Lv is a function. By definition

$$\begin{aligned} (ad_v^* Lv, w) &= (Lv, dv w - dw v) \\ &= (dv^* Lv, w) - (Lv, dw v) \end{aligned}$$

and the conclusion comes from Stoke's theorem which states that (since v and w vanish on $\partial\Omega$)

$$(\operatorname{div}(Lv \otimes v), w) = -(Lv, dw.v).$$

□

It appears that the Euler equation (5) with $ad_v^* Lv = \operatorname{div} v Lv + dv^* Lv$ has been derived in [24] and subsequently [20] directly as the Euler-Lagrange equation for the kinetic energy by analytical means. This has been originally proved by Arnold in [3] for the motion of incompressible fluid which corresponds to the case $L = \operatorname{Id}$ with the constraint $\operatorname{div} v = 0$.

3.2. Conservation of Momentum in Lagrangian Coordinates. The Euler equation (5) is the evolution of the momentum in Eulerian coordinates. We recognize in this equation the momentum $M_t^e \doteq Lv_t$; the momentum in Eulerian coordinates evolves in time so as to balance the co-adjoint of the momentum thereby satisfying the associated Euler equation $\frac{dM_t^e}{dt} + ad_{v_t}^*(M_t^e) = 0$ for extremal paths. However, *the momentum in Lagrangian coordinates*, identified in the introduction as $M_t^l = Ad_{\phi_t}^*(M_t^e)$, remains constant in the absence of external forces, $\frac{d}{dt} M_t^l = 0$.

¹These arguments are purely formal since h_t includes the Lie bracket which cannot be guaranteed to belong to \mathfrak{g} , in which case our variation would not be justified.

Statement 2. *Along extremal curves for the kinetic energy, M_t^l is constant:*

$$\frac{dM_t^l}{dt} = 0. \quad (7)$$

In particular, we have for all $w \in \mathfrak{g}$,

$$(Lv_t, w) = (Lv_0, (d\phi_t)^{-1}w \circ \phi_t). \quad (8)$$

Formal Derivation. Indeed, fix $w \in \mathfrak{g}$ and let $f(\varepsilon) = (M_{t+\varepsilon}^l, w)$. We have, on the first hand $f'(0) = \left(\frac{dM_t^l}{dt}, w\right)$, and on the second hand (derivatives being evaluated at time $\varepsilon = 0$)

$$f'(0) = \frac{d}{d\varepsilon}(Lv_{t+\varepsilon}, Ad_{\phi_{t+\varepsilon}}w) = \left(\frac{dLv_t}{dt}, Ad_{\phi_t}w\right) + \left(Lv_t, \frac{d}{d\varepsilon}Ad_{\phi_{t+\varepsilon}}w\right)$$

Note here that $Ad_{\phi_0 \circ \phi'} = Ad_{\phi} Ad_{\phi'}$. Now, if $\phi_0 = \text{id}$ and $\frac{d\phi_\varepsilon}{d\varepsilon} = v$ at $\varepsilon = 0$, we have for any w' ,

$$\frac{d}{d\varepsilon}(Ad_{\phi_\varepsilon}w')|_{\varepsilon=0} = \frac{d}{d\varepsilon}((d\phi_\varepsilon)w' \circ \phi_\varepsilon^{-1})|_{\varepsilon=0} = dv(w') - dw'(v) = ad_v w'. \quad (9)$$

Applying this to $w' = Ad_{\phi_t^{-1}}w$ and $v = v_t$, we get

$$f'(0) = \left(\frac{dLv_t}{dt}, Ad_{\phi_t}w\right) + (Lv_t, ad_{v_t} Ad_{\phi_t}w) = \left(\frac{dLv_t}{dt} + ad_{v_t}^* Lv_t, Ad_{\phi_t}w\right) = 0$$

by equation (5). This completes the proof,

$$\left(\frac{dM_t^l}{dt}, w\right) = 0.$$

□

Although the conservation of momentum has only been derived from formal arguments, we can check that, when it is satisfied, the generated deformation paths do provide extremal curves of the kinetic energy. The perturbation of the end point of the path $(\phi_{0t}^v, t \in [0, 1])$ at time 1 under a perturbation v_t^ε of v_t is given by [20]:

$$\frac{d}{d\varepsilon}\phi_{01}^{v^\varepsilon}(x) = \int_0^1 d_{\phi_{0s}^v} \phi_{s1}^v (h_s \circ \phi_{0s}^v) ds. \quad (10)$$

with $h_s(x) = \frac{dv_s^\varepsilon(x)}{d\varepsilon}$, the derivative being taken at $\varepsilon = 0$ (we have used the notation of equation (2)).

Assume that this expression vanishes (so that the end point $\phi_{01}^{v^\varepsilon}$ remains unchanged). The first

variation of the kinetic energy is given by $\int_0^1 \langle v_t, h_t \rangle_L dt = \int_0^1 (Lv_t, h_t) dt = \int_0^1 (Lv_0, d_{\phi_{0t}} \phi_{t0} v_t \circ \phi_{0t}) dt$.

Now, using (10) and the fact that $d_{\phi_{0t}} \phi_{t1} = d_{\phi_{00}} \phi_{01} d_{\phi_{0t}} \phi_{t0}$, we get easily that $\int_0^1 d_{\phi_{0t}} \phi_{t0} v_t \circ \phi_{0t} dt =$

0 so that, by linearity,

$$\int_0^1 \langle v_t, h_t \rangle_L dt = (Lv_0, \int_0^1 d_{\phi_{0t}} \phi_{t0} h_t \circ \phi_{0t} dt) = 0. \quad (11)$$

3.3. Coadjoint transport of structures along a geodesic. For $M \in \mathfrak{g}^*$, the evolution $t \mapsto Ad_{\phi_t}^* M$ is called coadjoint transport. The fact that the momentum evolves by coadjoint transport along a geodesic implies the conservation of several properties whenever they are initially true, for Lv_0 . These properties will turn out to be of main importance for image processing applications.

In this section, we assume that $M_0^e = Lv_0$ is given, and that the coadjoint transport $M_t^e = Lv_t = Ad_{\phi_{0t}}^*(Lv_0)$ is well defined at all considered times.

3.3.1. Coadjoint evolution of the support. Denote $\text{Supp}(v_0)$ the support of the initial momentum Lv_0 . It is defined by the complementary of the union of all open sets $\Omega' \in \Omega$ which are such that $(Lv_0, w) = 0$ whenever $w \in \mathfrak{g}$ vanishes outside Ω' . We have the property:

Statement 3. *If $M_t^e = Ad_{\phi_{0t}}^*(M_0^e)$, then*

$$\text{Supp}(v_t) = \phi_{0t}^v(\text{Supp}(v_0))$$

Indeed, assume that M_0^e vanishes on $\Omega' \subset \Omega$. Let w have its support included in $\phi_t(\Omega')$. Then $(M_t^e, w) = (M_0^e, (d\phi_t)^{-1}w \circ \phi_t)$ and $w \circ \phi_t$ vanishes outside Ω' , which implies that $(M_t^e, w) = 0$. Thus $\text{Supp}(Lv_t) \subset \phi_{0t}(\text{Supp}(M_0^e))$, and the reverse inclusion is true by inverting the roles of M_0^e and M_t^e .

As a first example, consider the case when M_0^e is finitely supported, and more precisely a sum of Dirac measures. This is legitimate since our hypotheses on L imply that Dirac measures belong to \mathfrak{g}^* , therefore have the form Lv_0 for some $v_0 \in \mathfrak{g}$.

$$(M_0^e, w) = \sum_i \langle a_i, w(x_i) \rangle_{\mathbb{R}^d}, \tag{12}$$

where $(x_i)_{1 \leq i \leq n}$ is a finite family of points in Ω (landmarks) and $(a_i)_{1 \leq i \leq n}$ is a finite family of vectors in \mathbb{R}^d . We write $M_0^e = \sum_{i=1}^n \delta_{x_i}^* a_i$, where, by definition

$$\begin{aligned} \delta_x^* a : \mathfrak{g} &\rightarrow \mathbb{R} \\ w &\mapsto \langle a, w(x) \rangle \end{aligned} \tag{13}$$

Denoting $x_i(t) \doteq \phi_t(x_i)$, we obtain the fact that M_t^e is supported on $\{x_1(t), \dots, x_N(t)\}$. More precisely, a rapid computation shows that

$$Lv_t = \sum_{i=1}^n \delta_{x_i(t)}^* a_i(t) \tag{14}$$

with

$$a_i(t) = (d_{x_i(t)}\phi_{t_0})^* a_i \quad (15)$$

so that the momentum remains a sum of Dirac measures. This is a special case of the property considered in the next section.

3.3.2. *Coadjoint transport of measure.* Measure-based momenta are given by

$$(M, w) = \int_{\Omega} \langle \nu_0, w \rangle d\mu_0 \quad (16)$$

where μ_0 is a measure on Ω and ν_0 is measurable and μ_0 -integrable. They generate a large class of geodesic evolution, and have the attractive property that the momentum $L\nu_t$ can be explicitly computed from the momentum at the origin.

Statement 4. *Assume that $(L\nu_0, w) = \int_{\Omega} \langle \nu_0, w \rangle d\mu_0$, then the linear momentum functional evolves according to*

$$(L\nu_t, w) = \int_{\Omega} \langle \nu_t, w \rangle_{\mathbb{R}^d} d\mu_t \text{ where } \nu_t(x) = d_x(\phi_{t_0})^* \nu_0 \circ \phi_{t_0}(x), \mu_t \doteq \mu \circ \phi_{t_0}, \quad (17)$$

ie. $\mu_t(A) = \mu(\phi_{t_0}(A))$ for any measurable set A .

The statement follows straightforwardly from the substitutions

$$\begin{aligned} (L\nu_t, w) &= \int_{\Omega} \langle \nu_0(x), ((d\phi_{0t})^{-1} w \circ \phi_{0t})(x) \rangle_{\mathbb{R}^d} d\mu(x) = \int_{\Omega} \langle d_{\phi_{0t}(x)}\phi_{t_0}^* \nu_0(x), w \circ \phi_{0t}(x) \rangle_{\mathbb{R}^d} d\mu_0(x) \\ &= \int_{\Omega} \langle \nu_t(x), w(x) \rangle_{\mathbb{R}^d} d\mu_t(x) \end{aligned} \quad (18)$$

Point-supported momentum evolution considered in the previous section, clearly is a particular case of this statement. As another illustration, consider the case of measures which are supported by submanifolds of Ω . In this case, the initial momentum is concentrated along the boundary Σ_0 of a k -dimensional C^1 sub-manifold in $\Omega \subset \mathbb{R}^d$.

Let σ_0 be the surface measure (given as the induced volume form on the sub-manifold) and let μ_0 be supported by Σ_0 such that for any smooth function on Ω , $\int_{\Omega} f d\mu_0 = \int_{\Sigma_0} f \alpha_0 d\sigma_0$ for some density α_0 (not necessary positive) on the surface. Let $\nu_0 : \Omega \rightarrow \mathbb{R}^d$ (the values of ν_0 outside Σ_0 will not be important) and define

$$(L\nu_0, w) = \int_{\Sigma_0} \langle \nu_0, w \rangle_{\mathbb{R}^d} \alpha_0 d\sigma_0. \quad (19)$$

Using Statements 3 and 4, we get that the transported measure μ_t is located on the transported sub-manifold $\Sigma_t \doteq \phi_t(\Sigma_0)$ (whose smoothness is preserved by the regularity of the diffeomorphisms in G) and can be written as $\mu_t = \alpha_t \sigma_t$ where σ_t is the k -dimensional volume measure on Σ_t . Moreover, if $\nu_t = d(\phi_{t0})^* \alpha_0 \circ \phi_{t0}$, Statement 4 gives us the evolution of the momentum

$$(Lv_t, w) = \int_{\Sigma_t} \langle \nu_t, w \rangle \alpha_t d\sigma_t(y). \quad (20)$$

In the case where the sub-manifold is Ω itself, then $\sigma_t = \sigma_0$ is the Lebesgue's measure λ on Ω , and $\alpha_t = \alpha_0 \circ \phi_{t,0} |d\phi_{t,0}|$.

3.3.3. Coadjoint transport of orthogonality. The last property transported by geodesic evolution which is considered here is the normality with respect to a smooth submanifold of Ω . Since normality will be extensively studied in the next section, we here provide an illustration in a particular case.

Assume that ν_0 , in equation (16) can be expressed as

$$\nu_0 = \sum_{i=1}^r b_0^i \nabla f_0^i \quad (21)$$

where $(b_0^i)_{1 \leq i \leq r}$ and (f_0^i) are two families of functions on Ω and $1 \leq r \leq d$. Then, we get from Statement 4 that

$$\nu_t = \sum_{i=1}^r b_t^i \nabla f_t^i \quad (22)$$

where $b_t^i = b_0^i \circ \phi_{t,0}$ and $f_t^i = f_0^i \circ \phi_{t,0}$. Equation (22) can be interpreted as a normality property of the geodesic motion under initial condition (21). Indeed, let

$$\Sigma_0 = \bigcap_{i=1}^r (f_0^i)^{-1}(\{0\}).$$

Assume that Σ_0 is not empty and denotes $N_0(x) = \text{Span}\{\nabla f_0^i(x) \mid 1 \leq i \leq r\}$ for any $x \in \Sigma_0$.

Under appropriate transversality conditions, mainly

$$r \equiv \dim N_0,$$

Σ_0 can be equipped with a structure of $(d-r)$ -dimensional C^1 manifold and $N_0(x)$ is exactly the space of vectors normal to Σ_0 at location x .

We then deduce easily that

$$\Sigma_t = \bigcap_{i=1}^r (f_t^i)^{-1}(\{0\})$$

and equality (22) implies for any $x \in \Sigma_t$

$$\nu_t(x) \in N_t(x) \tag{23}$$

where $N_t(x) = \text{Span}\{\nabla f_t^i(x) \mid 1 \leq i \leq r\}$ is the set of normal vectors to Σ_t at location x .

We deduce that if the momentum is normal to some k -dimensional sub-manifold Σ_0 , this normality property is preserved by coadjoint transport along a geodesic.

In the case of $r = 1$ and $f_0^1 = f_0$, Σ_0 is exactly the level set for threshold value 0 of f_0 and the normality of the initial momentum to the level sets is preserved under geodesic motion. Since the threshold value is arbitrary, we deduce that the property is true for any level sets.

4. THE NORMAL MOMENTUM MOTION CONSTRAINT

4.1. Heuristic analysis. The conservation of momentum is a general property of geodesics in a group of diffeomorphisms with a right invariant metric. More can be said in the situation when diffeomorphisms are associated to deformations of geometric structures or images, which is the situation of interest for our applications. In this setting we are still looking for curves with shortest length in G , but we relax the fixed end-point condition by the constraint that the initial template is correctly mapped to the target: because there is a whole range of diffeomorphisms which deform one given structure into another, this condition is weaker than the fixed end-point condition, which means that there are more degree of freedom for the optimization, and therefore more constraints on the minimum. For image matching, these additional constraints may essentially be summarized by the statement *the momentum along the geodesic path is at all times normal to the level sets of the image*. This is what we call the *normal momentum constraint*, which is described in this section.

We start with a heuristic analysis, for which I_0 , the image, is a smooth function defined on Ω . Let I_1 be in the orbit of I_0 for the group G of diffeomorphisms: there exists $\psi \in G$ such that $I_0 \circ \psi = I_1$. By compactness and semi-continuity arguments, one can prove the existence of a

geodesic path $\phi = (\phi_t)$ such that

$$d_G(\text{Id}, \phi_1) = \inf_{\varphi \in G} d_G(\text{Id}, \varphi) \quad \text{and} \quad I_0 = I_1 \circ \varphi. \quad (24)$$

Let $\phi = (\phi_t^v)$ be such a solution and consider a first order expansion around $t = 0$, $\phi_t(x) \simeq x + tv_0(x)$ so that $I_t = I_0 \circ \phi_t^{-1}(x) \simeq I_0 - t\langle \nabla I_0, v_0 \rangle_L$. By definition, the cost to go from I_0 to I_t is (still at first order) $t|v_0|_L$. However, any $u \in \mathfrak{g}$ such that $\langle \nabla I_0, u \rangle_{\mathbb{R}^d} = \langle \nabla I_0, v_0 \rangle_{\mathbb{R}^d}$, will lead to the same I_t so that the least deformation cost from I_0 to I_t should be $t|p_{I_0}(v_0)|$ where $p_{I_0}(v_0)$ the unique solution of the minimization problem:

$$(\mathcal{P}_0) : \inf_{u \in \mathfrak{g}} |u|_L \quad \text{subject to:} \quad \langle (v_0 - u)(x), \nabla I_0(x) \rangle_{\mathbb{R}^d} = 0, \quad \forall x \in \Omega \quad (25)$$

Since (ϕ_t^v) is a geodesic path minimizing the deformation cost from I_0 to I_1 , it minimizes also the deformation cost from I_0 to I_t yielding

$$v_0 = p_{I_0}(v_0). \quad (26)$$

Introduce the set $\mathfrak{g}_{I_0} = \{ h \in \mathfrak{g} \mid \langle \nabla I_0(x), h(x) \rangle_{\mathbb{R}^d} = 0, \forall x \in \Omega \}$: the constraints in \mathcal{P}_0 can be restated as $u - v_0 \in \mathfrak{g}_{I_0}$ so that $p_{I_0}(v)$ is the orthogonal projection of v on $\mathfrak{g}_{I_0}^\perp$, the space orthogonal to \mathfrak{g}_{I_0} . Hence, equality (26), translates to

$$\forall h \in \mathfrak{g} \text{ such that for all } x \in \Omega \langle \nabla I_0(x), h(x) \rangle = 0, \quad \text{we have } \langle v_0, h \rangle_L = 0. \quad (27)$$

Now, the fact that $\langle \nabla I_0(x), h(x) \rangle \equiv 0$ means that h is a vector field which is tangent to the level sets of I_0 , and since $\langle v_0, h \rangle_L = (Lv_0, h)$, we see that Lv_0 vanishes when applied to any such vector field, or, that Lv_0 is a linear form which is normal to the level sets of I_0 .

4.2. Rigorous result. We now pass to a rigorous derivation of this property. Since it will be interesting to also consider images which are not smooth, we provide a new definition of the set \mathfrak{g}_{I_0} . Obviously, when I_0 is smooth, $h \in \mathfrak{g}_{I_0}$ is equivalent to the fact that, for any function f which is C^1 on Ω , one has

$$\int_{\Omega} \langle \nabla_x I_0, h(x) \rangle_{\mathbb{R}^k} f(x) dx = 0$$

Applying the divergence theorem (we assume that $\partial\Omega$ is smooth enough and take advantage on the fact that elements of \mathfrak{g} vanish on $\partial\Omega$), we get

$$-\int_{\Omega} I_0(x) \operatorname{div}(hf)(x) dx = 0$$

Since this has a meaning when $I_0 \in L^2(\Omega)$, we now define

Definition 2. When $I \in L^2(\Omega)$, we denote

$$\mathfrak{g}_I = \{h \in \mathfrak{g} : \langle I, \operatorname{div}(hf) \rangle_{L^2} = 0 \text{ for all } f \in C^1(\Omega)\}$$

We still denote by p_I the orthogonal projection on \mathfrak{g}_I^\perp . The group G is assumed to be built as described in section 2.1 (in particular \mathfrak{g} is continuously embedded in $C^1(\Omega, \mathbb{R}^d)$).

Theorem 1 (Normal Momentum Constraint). *Assume that $I_0 \in L^2(\Omega)$ and let $\phi = (\phi_t^v)$ be a geodesic path solution of (24). Then, for almost all $t \in [0, 1]$*

$$v_t \in \mathfrak{g}_{I_t}^\perp.$$

Proof. Since $\mathfrak{g}_{I_t}^\perp$ is closed, we have to show that for almost all t , $v_t = p_{I_t}(v_t)$. Denote $h_t \doteq v_t - p_{I_t}(v_t)$. For $\varepsilon \in [0, 1]$, let $v_t^\varepsilon \doteq v_t + \varepsilon h_t$, and $\phi_t^\varepsilon \doteq \phi_t^{v_t^\varepsilon}$ (one can check, but we skip the argument, that $t \rightarrow h_t$ is measurable and belongs to $L^2([0, 1], \mathfrak{g})$, so that this variation is valid).

The proof essentially consists in showing that, for all $0 \leq t \leq 1$

$$I_0 \circ \phi_{t0} = I_0 \circ \phi_{t0}^\varepsilon. \quad (28)$$

Indeed, assume that this result is proved. Considering $\varepsilon = 1$ and $t = 1$, we deduce that $I_1 = I_0 \circ \phi_{1,0}^1$. However, since $\langle h_t, v_t \rangle_L = \langle v_t - p_{I_t}(v_t), v_t \rangle_L = 0$, we get $|v_t + h_t|_L^2 = |v_t|_L^2 - |h_t|_L^2$. Since $t \rightarrow v_t$ corresponds to paths with lowest kinetic energy from I_0 to I_1 , we deduce that $\int_0^1 |h_t|_L^2 = 0$ and the proof is ended.

We now return to equation (28). Using the formula

$$\frac{d\phi_{t0}(x)}{dt} = -d_x \phi_{t0} v_t(x)$$

and letting $q_t^\varepsilon(x) = \phi_{t0} \circ \phi_{0t}^\varepsilon(x)$, we obtain

$$\begin{aligned} \frac{\partial q_t^\varepsilon(x)}{\partial t} &= -d_{\phi_{0t}^\varepsilon(x)} \phi_{t0} v_t \circ \phi_{0t}^\varepsilon(x) + d_{\phi_{0t}^\varepsilon(x)} \phi_{t0} (v_t \circ \phi_{0t}^\varepsilon(x) + \varepsilon h_t \circ \phi_{0t}^\varepsilon(x)) \\ &= \varepsilon d_{\phi_{0t}^\varepsilon(x)} \phi_{t0} h_t \circ \phi_{0t}^\varepsilon(x) \end{aligned}$$

We first prove equation (28) under the assumption that I_0 is C^1 . From the computation above, we have

$$\begin{aligned} \frac{\partial}{\partial t} (I_0 \circ q_t^\varepsilon)(x) &= \varepsilon \langle \nabla_{\phi_{t0}(\phi_{0t}^\varepsilon(x))} I_0, d_{\phi_{0t}^\varepsilon(x)} \phi_{t0} h_t \circ \phi_{0t}^\varepsilon(x) \rangle_{\mathbb{R}^d} \\ &= \varepsilon \langle \nabla_{\phi_{0t}^\varepsilon(x)} I_t, h_t(\phi_{0t}^\varepsilon(x)) \rangle_{\mathbb{R}^d} = 0 \end{aligned}$$

since by definition of the projection $p_{I_t}(v_t)$, we have for any $x \in \Omega$

$$\langle h_t(x), \nabla I_t(x) \rangle_{\mathbb{R}^d} = \langle v_t(x), \nabla I_t(x) \rangle_{\mathbb{R}^d} - \langle p_{I_t}(v_t), \nabla I_t(x) \rangle_{\mathbb{R}^d} = 0.$$

This implies $I_0 \circ \phi_{t,0} \circ \phi_{0,t}^\varepsilon = I_0$ which yields equation (28) in this case. When I_0 is not smooth, the proof goes by showing that

$$\frac{\partial}{\partial t} \int_{\Omega} I_0 \circ q_t^\varepsilon(x) f(x) dx = \int_{\Omega} I_t(x) \operatorname{div}(h_t g_t^\varepsilon)(x) dx$$

for smooth f on Ω and $g_i^\varepsilon \circ \phi_i^\varepsilon |d\phi_i^\varepsilon| = f$, which can be done either by a direct (heavy) computation, or by using a density argument, based on the fact that, by the divergence theorem, this is true for smooth I_0 (we skip the details). \square

4.3. Examples. Consider again the case of smooth I , so that the condition $h \in \mathfrak{g}_I$ is equivalent to $h \in \mathfrak{g}$ and for all $x \in \Omega$, $\langle \nabla_x I, h(x) \rangle_{\mathbb{R}^d} = 0$. Using notation (13), we get that $\langle \nabla I_0(x), h(x) \rangle_{\mathbb{R}^d} = \langle \delta_x^*(\nabla I_0(x)), h \rangle_L$ so that $\mathfrak{g}_{I_0} = (\text{Span}\{ \delta_x^*(\nabla I_0(x)) \mid x \in \Omega \})^\perp$ and finally,

$$\mathfrak{g}_I^\perp = \overline{\text{Span}\{ \delta_x^*(\nabla I(x)) \mid x \in \Omega \}}. \quad (29)$$

Moments of the kind

$$(Lv, u) = \int_{\Omega} \langle \nu(x), u(x) \rangle_{\mathbb{R}^d} d\mu(x). \quad (30)$$

where ν is normal² to the level sets of I belong to \mathfrak{g}_I^\perp and it can be shown that they form a dense subset.

For non-smooth I , we can similarly introduce $\omega_f(I)$, as the unique element of \mathfrak{g} such that, for $h \in V$, $\langle \omega_f(I), h \rangle = \langle I, \text{div}(hf) \rangle_{L^2(\Omega)}$, and conclude that

$$\mathfrak{g}_I^\perp = \overline{\text{Span}\{ \omega_f(I) \mid f \in C^1(\Omega, \mathbb{R}) \}}. \quad (31)$$

This implies that any element $v \in \mathfrak{g}_I$ can be expressed as a limit

$$(Lv, u) = \lim_{N \rightarrow \infty} \int_{\Omega} I(x) \text{div}(u f_N)(x) dx$$

where $f_N \in C^1(\Omega, \mathbb{R})$. The particular case when I is the indicator function of a smooth domain $B \subset \Omega$ (which can be interpreted as a smooth shape) is quite interesting. For $x \in \partial B$, let $\nu(x)$ be the outward normal to $\partial\Omega$ and denote σ_B be the uniform measure on ∂B . Then

$$\int_{\Omega} I(x) \text{div}(uf)(x) = \int_B \text{div}(uf)(x) = \int_{\partial B} f(x) \langle u(x), \nu(x) \rangle_{\mathbb{R}^d} d\sigma_B(x).$$

In this case, we obtain a dense subspace of \mathfrak{g}_I by considering elements $v \in \mathfrak{g}$ given by

$$(Lv, u) = \int_{\partial B} \langle \nu(x), u(x) \rangle_{\mathbb{R}^d} d\mu(x). \quad (32)$$

for some measure μ on ∂B (the boundary of the shape).

²When I has smooth level sets, we say that a vector field ν is normal to its level sets when, denoting by Ω_i the set $\{I \leq i\}$, $\nu(x)$ is normal to $\partial\Omega_i$ if $x \in \partial\Omega_i$ for some i and $\nu(x) = 0$ otherwise.

Remark. We close this section with an important remark. We have called *normal momentum constraint* the property that $v_t \perp \mathfrak{g}_{I_t}$ at almost all times. We have shown that this property is always true for geodesics minimizing (24), but we did not analyze how much it constrains v_t , asking the question: how big is \mathfrak{g}_I for a given image I . That this issue is highly relevant may be seen from the following example: assume that we are in 2 dimensions ($d = 2$) and that I is a C^1 image, with a non-vanishing gradient, at least on a dense subset of Ω . Then, on any point x such that $\nabla_x I \neq 0$, we can define in a unique way a positively oriented orthonormal frame $(\tau(x), \nu(x))$ such that $\nu(x) = \nabla_x I / |\nabla_x I|$. Then, if $h \in \mathfrak{g}_I$ and $h(x) \neq 0$, we must have $h/|h| = \pm\tau$ in a small ball around x . Now h , as an element of \mathfrak{g} must be smooth (depending on the choice made for L), and $h/|h|$ has the same smoothness as h : this is impossible to achieve when τ itself is not smooth enough, which in such a case forces $h(x) = 0$. We thus get the property that h vanishes whenever $\tau(x)$ does not meet the smoothness requirements of \mathfrak{g} , which may very well be everywhere on Ω (or on a dense subset, which is the same since h is continuous), in which case $\mathfrak{g}_I = \{0\}$ and the constraint is void. We see that, for the constraint to really be effective, we need some smoothness requirement on I . Fortunately, as illustrated by the example above, this smoothness is only required for the *level sets* of I , which must have a smooth boundary. With such an assumption, for example, one can show that if $v \perp \mathfrak{g}_I$ and

$$(Lv, u) = \int_{\Omega} \langle \xi(x), u(x) \rangle d\mu(x)$$

for some measure μ on Ω and some vector field ξ on Ω , then ξ must be (μ -almost everywhere) orthogonal to the level sets of I . From a practical point of view smoothness of level sets may easily be obtained using algorithms such as mean curvature motion ([25]).

4.4. Conservation and Normality Property Check For Inexact Matching. Here, we give a brief account of situations in which proofs of conservation of momentum and the normality property can be carried on in a well-defined context, and retrieve the evolutions described in the previous section.

It is hard to make rigorous, in full generality, the variational argument we have used in the proof of equation (5). Notice that the well-definiteness of the conservation of momentum equation (7) is an issue by itself, since, when $w \in \mathfrak{g}$, and ϕ_t is the diffeomorphism generated by a geodesic, there is a priori no reason for $(d\phi_t)^{-1}w \circ \phi_t$ to belong to \mathfrak{g} : one must be able to define Lv_0 on spaces which are bigger than \mathfrak{g} , which means that Lv_0 needs to be somewhat smoother (as a distribution) than a generic element of \mathfrak{g}^* .

However, there is a setting in which such a fact is true and easy to obtain: it is when the search for the geodesic is done with an approximation of the target, with some L^2 penalty term added to control the error. We summarize this setting in the case of image matching, shape matching and landmark matching. In these three situations, we will retrieve the coadjoint transport of

measure-based momenta. In all cases, results in [33, 9] ensure the existence of minimizers of the variational problem.

4.4.1. *Inexact landmark matching.* In this section, we assume that a measured space (\mathcal{J}, ρ) , together with two measurable functions $x, y : \mathcal{J} \rightarrow \Omega$ are given. The diffeomorphism ϕ is searched to minimize

$$U(\phi) = E(\phi) + \frac{1}{\sigma^2} \int_{\mathcal{J}} |y_i - \phi(x_i)|^2 d\rho(i)$$

When ρ is discrete, this relates to point-based matching, x representing the landmark original positions and y giving the landmark target positions. If we express U in function of v , this requires the minimization of

$$\tilde{U}(v) = \int_0^1 \|v_t\|_L^2 dt + \frac{1}{\sigma^2} \int_{\mathcal{J}} |y_i - \phi_{01}^v \circ x_i|^2 d\rho(i)$$

The main point here is to notice that the optimal solution v generates a geodesic in G between id and ϕ_1^v .

Proposition 1. *Denote $\delta_x^* a$ the linear form on \mathfrak{g} such that $(\delta_x^* a, v) = \langle a, v(x) \rangle$. Let v be a minimizer of \tilde{U} . Then, letting $x_i(t) = \phi_{0t}^v(x_i)$*

$$Lv_t = -\frac{1}{\sigma^2} \int_{\mathcal{J}} \delta_{x_i(t)}^* [(d_{x_i(t)} \phi_{t1}^v)^*(y_i - x_i(1))] d\rho(i) \quad (33)$$

Proof. The proof of this result is a direct consequence of the identity, valid for $s, t \in [0, 1]$, $v, h \in L^2([0, 1], \mathfrak{g})$,

$$\frac{d}{d\varepsilon} \phi_{st}^{v+\varepsilon h}(x)|_{\varepsilon=0} = \int_s^t d_{\phi_{su}^v} \phi_{ut}^v(h_u \circ \phi_{su}^v) du. \quad (34)$$

the proof of which being carried on with usual ODE arguments and being omitted here. It is then straightforward to obtain (33), using the definition of the linear forms $\delta_x^* a$, for $x \in \Omega$ and $a \in \mathbb{R}^d$. \square

Equation (33) is a conservation of momentum equation for

$$Lv_0 = -\frac{1}{\sigma^2} \int_{\mathcal{J}} \delta_{x_i}^* [(d_{x_i} \phi_{01}^v)^*(y_i - x_i(1))] d\rho(i).$$

When \mathcal{J} is finite, this is equation (21) with $a_i = -\frac{1}{\sigma^2}(d_{x_i}\phi_{01}^v)^*(y_i - x_i(1))$. Equation (33) now is exactly (14), since

$$\begin{aligned} a_i(t) &= (d_{x_i(t)}\phi_{t,0}^v)^* a_i \\ &= -\frac{1}{\sigma^2} [d_{x_i(0)}\phi_{01}^v d_{x_i(t)}\phi_{t,0}^v]^* (y_i - x_i(1)) \\ &= -\frac{1}{\sigma^2} (d_{x_i(t)}\phi_{t,1}^v)^* (y_i - x_i(1)) \end{aligned}$$

4.4.2. Inexact shape matching. We now consider the comparison of a binary set-indicator function, $I_0 = \mathbf{1}_{\Omega_0}$ ($\overline{\Omega_0} \subset \Omega$ having smooth boundaries) and a smooth function I_1 , through the minimization of

$$U(\phi) = E(\phi) + \frac{1}{\sigma^2} \int_{\Omega} |\mathbf{1}_{\Omega_0} \circ \phi^{-1}(x) - I_1(x)|^2 dx$$

over G_L . We have

Proposition 2. *Let v be a minimizer of $U(\phi_{01}^v)$ over $L^2([0, 1], \mathfrak{g})$. Then*

$$Lv_t = \frac{1}{\sigma^2} \int_{\partial\Omega_1} \left(\frac{1}{2} - I_1 \right) \delta_{\phi_{t1}^v(x)}^* [(d_{\phi_{t1}^v} \phi_{t1}^v)^* \nu_1] d\sigma_1(x) \quad (35)$$

where $\Omega_1 = \phi_{01}^v(\Omega_0)$, ν_1 is the outward normal to $\partial\Omega_1$ and σ_1 is the volume measure on $\partial\Omega_1$.

Proof. Taking a variation $v + \varepsilon h$, the main issue is to compute the derivative of

$$\frac{1}{2} \int_{\Omega} |\mathbf{1}_{\Omega_0} \circ \phi_{10}^{v+\varepsilon h}(x) - I_1(x)|^2 dx$$

This integral can be rewritten

$$\int_{\phi_{01}^{v+\varepsilon h}(\Omega_0)} \left(\frac{1}{2} - I_1(x) \right) dx + \frac{1}{2} \int_{\Omega} |I_1(x)|^2 dx$$

Since the last term is constant, we see that the problem boils down to the computation of the derivative of the first term, which can be written, after a change of variable and letting $f_1 = 1/2 - I_1$,

$$\int_{\Omega_0} f_1 \circ \phi_{01}^{v+\varepsilon h}(x) |d_x \phi_{01}^{v+\varepsilon h}| dx$$

Define u by $u \circ \phi_{01}^v(x) = \frac{d}{d\varepsilon} \phi_{01}^{v+\varepsilon h}(x)$. Simple computations, which can be, for example, found in [8], yields the fact that

$$\frac{d}{d\varepsilon} \int_{\Omega_0} f_1 \circ \phi_{01}^{v+\varepsilon h}(x) |d_x \phi_{01}^{v+\varepsilon h}| dx = \int_{\Omega_1} \operatorname{div}(f_1 u) dx$$

Now the conclusion is a direct consequence of equation (34) and of the divergence theorem. \square

Here again, one straightforwardly checks that the conservation of momentum is satisfied. We have in particular

$$(Lv_0, w) = \frac{1}{\sigma^2} \int_{\partial\Omega_1} \left(\frac{1}{2} - I_1 \right) \langle (d_{\phi_{10}^v} \phi_{01}^v)^* \nu_1, w \circ \phi_{10}^v(x) \rangle d\sigma_1(x)$$

Letting $\mu_0 = \phi_{01}^v(\sigma_1)$, and $\nu_0(x) = (d_x \phi_{01}^v)^* \nu_1 \circ \phi_{10}^v(x)$, this can be rewritten

$$(Lv_0, w) = \frac{1}{\sigma^2} \int_{\partial\Omega_0} \left(\frac{1}{2} - I_1 \circ \phi_{01}^v(x) \right) \langle \nu_0, w \rangle d\mu_0(x)$$

which is under the general form of a measure-based momentum.

4.4.3. Inexact image matching. In this section, we let I_0 and I_1 be two smooth enough (say C^1) functions defined on Ω (images). We consider the image matching problem which corresponds to minimizing, over G ,

$$U(\phi) = E(\phi) + \frac{1}{\sigma^2} \int_{\Omega} |I_0 \circ \phi^{-1}(x) - I_1(x)|^2 dx$$

This problem is equivalent to minimizing

$$\int_0^1 \|v_t\|_L^2 dt + \frac{1}{\sigma^2} \int_{\Omega} |I_0 \circ (\phi_{01}^v)^{-1}(x) - I_1(x)|^2 dx$$

This matching problem has been studied, in particular in (cite Beg etc...), to show that the optimal solution should satisfy, at each time t ,

$$Lv_t = -\frac{1}{\sigma^2} |d\phi_{t,1}^v| (I_{0t}^v - I_{1t}^v) \nabla I_{0t}^v \quad (36)$$

in which we have introduced the notation: $I_{0t}^v = I_0 \circ \phi_{t0}^v$, $I_{1t}^v = I_1 \circ \phi_{t1}^v$, and $|d\phi|$ for the Jacobian of ϕ . This equation is in fact an equation of conservation of momentum, with

$$Lv_0 = -\frac{1}{\sigma^2} |d\phi_{01}^v| (I_0 - I_{10}^v) \nabla I_0$$

as can be deduced from equation (20), with $\alpha = -\frac{1}{\sigma^2} |d\phi_{01}^v| (I_0 - I_{10}^v)$. Moreover, we can check also the normality property (21) which holds here with with $r = 1$ and $f_0 = I_0$. This allow us to conclude that for the geodesic path in the image space generated by inexact matching, the lifting of the path in G defines a geodesic for which the momentum stays normal to the level sets of the current image $I_0 \circ \phi_{t,0}$ at time t .

5. GEODESIC EVOLUTION IN THE ORBIT

Thus far we have concentrated on the evolution of the flow of diffeomorphisms and its conservation of momentum. For all of our image understanding work we use the flow $(\phi_t, t \in [0, 1])$ to act on the elements in the orbits \mathcal{J} of a given template $I = I_{\text{temp}}$. Now we examine the geodesic flows in the orbit $\{I_t = I \circ \phi_t, t \in [0, 1]\}$, $I \in \mathcal{J}$, and provide the associated evolution equations.

5.1. Geodesic Evolution Equation of Landmark Points. Here we examine the finite dimensional landmark orbit denoted \mathcal{J}_n , consisting of n -shapes $I_N = (x_1, \dots, x_n)$, each landmark $(x_i)_{1 \leq i \leq n}$ is in $\Omega \subset \mathbb{R}^d$; correspondingly $(a_i)_{1 \leq i \leq n}$ are a finite family of vectors in \mathbb{R}^d . Denoting by $x_i(t) \doteq \phi_t(x_i)$, the trajectory in Ω of the point x_i under the flow ϕ_t gives

$$Lv_t = \sum_{i=1}^n \delta_{x_i(t)}^* a_i(t), \quad (37)$$

where $a_i(t) = (d_{x_i(t)} \phi_{t,0})^* a_i$. A straightforward computation giving

$$\frac{d}{dt}((d_{x_i(t)} \phi_{t,0})^*) = -d_{x_i(t)} v_t^* (d_{x_i(t)} \phi_{t,0})^*,$$

we deduce that $\frac{da_i}{dt}(t) + (d_{x_i(t)} v_t)^* a_i(t) = 0$. Hence we get the following geodesic evolution in the orbit of landmarks.

Proposition 3 (Landmark Transport). *The landmarks are transported along the geodesic according to the following equations with velocity vector field satisfying*

$$v_t = L^{-1} \left(\sum_{i=1}^n \delta_{x_i(t)}^* a_i(t) \right) = \sum_{i=1}^n K(x_i(t), \cdot) a_i(t)$$

where $K(x, y)$ is the Green kernel associated with L :³

$$\begin{cases} \frac{da_i}{dt}(t) + (d_{x_i(t)} v_t)^* a_i(t) = 0, \\ \frac{dx_i}{dt}(t) - v_t(x_i(t)) = 0. \end{cases} \quad (39)$$

Note that the expression of v_t from equation (38) can be introduced into the system (39), yielding an evolution equation which only depends on the landmarks in the orbit.

We notice the reduction of the vector field to the range space of the Green's kernels travelling over the landmark trajectories is as in [15].

There is a straightforward extension of this result to *geodesic curve evolution*, in which $x(0)$ is a parametrized curve $\sigma \mapsto x(\sigma)$ for $\sigma \in [0, L]$ and

$$Lv_0 = \int_0^L \delta_{x(0,\sigma)}^* \nu_0(\sigma) d\sigma$$

³The explicit form for L^{-1} depending on the kernel K is defined as follows. For any $x, y \in \Omega$, the bilinear form $K_{x,y}$ on $\mathbb{R}^d \times \mathbb{R}^d$ defined by

$$K_{x,y}(a, b) \doteq \langle \delta_x^* a, \delta_y^* b \rangle_{\mathfrak{g}^*} = \langle \delta_y^* b, L^{-1}(\delta_x^* a) \rangle = \langle L^{-1}(\delta_x^* a)(y), b \rangle_{\mathbb{R}^d} \quad (38)$$

where $\nu_0(\sigma)$ is normal to $x(0)$. In this case, we have

$$Lv_t = \int_0^L \delta_{x(t,\sigma)}^* \nu_t(\sigma) d\sigma$$

with

- $\frac{\partial \nu_t}{\partial t}(t, \sigma) + (d_{x(t,\sigma)} v_t)^* \nu(t, \sigma) = 0,$
- $\frac{\partial x}{\partial t}(t, \sigma) - v_t(x(t, \sigma)) = 0.$

5.2. Geodesic Image Evolution. Assume here that $d\mu = \alpha(x)dx$ has a density with respect to Lebesgue's measure on Ω . In this case, $d\mu_t = |d\phi_{t0}| \alpha \circ \phi_{t0} dx$ and

$$Lv_t = |d\phi_{t0}| \alpha \circ \phi_{t0} dI_t \quad (40)$$

From the conservation of momentum in Lagrangian coordinates for image based motion, we get for $Lv_0 = \alpha_0 \nabla I_0$, that $Lv_t = \alpha_t |d\phi_{t,0}| \nabla I_t$ where $\alpha_t = \alpha_0 \circ \phi_{t,0}$, $I_t = I_0 \circ \phi_{t,0}$. Let $z_t = \alpha_t |d\phi_{t,0}|$ so that $Lv_t = z_t \nabla I_t$.

Since $\frac{d}{dt}(z_t \circ \phi_{0,t}) = \frac{d}{dt}(|d\phi_{0,t}| \alpha_0) = -\text{div}(v_t) \circ \phi_{0,t} |d\phi_{0,t}| \alpha_0$, we get $\frac{dz_t}{dt} + dz_t(v_t) + \text{div}(v_t) z_t$. Moreover, we get easily $\frac{\partial I_t}{\partial t} + \langle \nabla I_t, v_t \rangle = 0$. Hence we get the following geodesic evolution equation in image space.

Proposition 4 (Image Transport). *The image is transported along the geodesic according to the following equations: with vector field $v_t = L^{-1}(z_t \nabla I_t)$:*

- $\frac{dz_t}{dt} + dz_t(v_t) + \text{div}(v_t) z_t = 0,$
- $\frac{\partial I_t}{\partial t} + \langle \nabla I_t, v_t \rangle = 0.$

Notice that these equations appear as a limit case of the evolution equations which have been studied in [32] for image comparison.

As illustrated above, the pair (I_0, μ) provides a device for modeling deformations. In the cases we have studied, I_0 was representing some geometrical structure (a curve, an image), which evolved with time according to the generated deformation, and μ , essentially quantifies the speed and direction of the deformation.

We get from this a natural way to represent the deformation of a template. Using Grenander’s original terminology, I_0 would precisely be the template and μ is the generator of the deformation. Thus, fixing I_0 , and letting μ vary, we get a model which represents perturbations of the template.

An example of deformations of an image is provided in figure 2. The images have been obtained by solving equation (40) from an initial image g of a slice of macaque brain, and taking

$$\alpha(x) = \frac{X(x)}{1 + |\nabla_x I_0|}$$

where X is a Gaussian process.



FIGURE 2. Three random deformations of an image.

6. COMPUTATIONAL RESULTS

Shown in Figures 3- 7 are results illustrating the image based momentum and the diffeomorphisms generated via geodesic shooting using Faisal Beg’s algorithms. Figures 3 shows the three objects studied, a smooth Gaussian bump for shift, circles for scale, and two mitochondria examining both forward and inverse shooting.

Shown in figure 4 are comparisons between momentum at the identity Lv_0 and the gradient of the image ∇I_0 . Shown superimposed at every point in the grid are the arrows depicting the direction vector of each.

Shown in Figures 5- 7 are examples illustrating the image based momentum and the diffeomorphisms generated via geodesic shooting. Figure 5 shows the results of the translation experiment. Panels 1 and 2 show I_0 and I_1 ; panel 3 shows the diffeomorphism generated via geodesic shooting applied to I_0 . Lv_0 was calculated using Faisal Beg’s matching algorithm for diffeomorphic matching of I_0 to I_1 and then that momentum at the origin was transported according to the

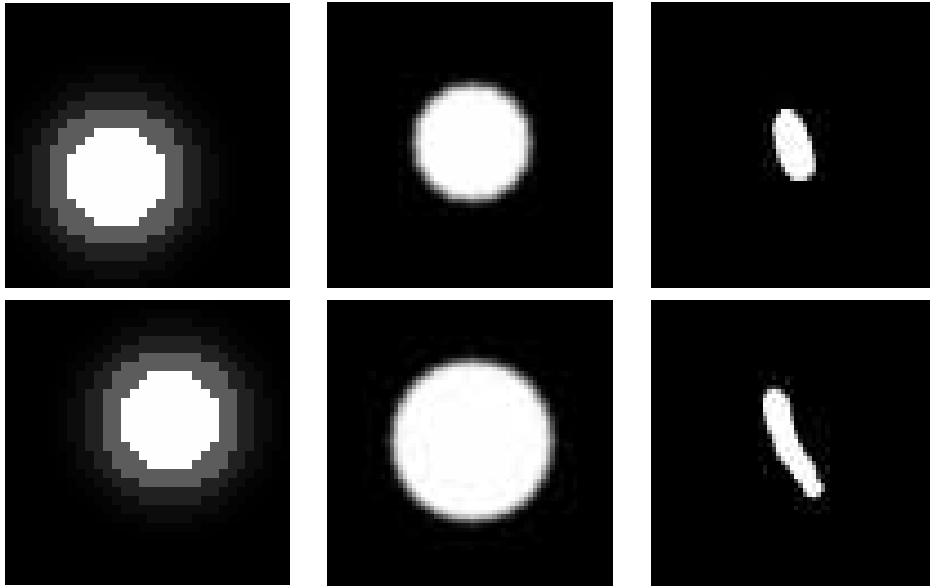


FIGURE 3. Figure shows objects under translation (column 1), scale (column 2), and mitochondria 1 and 2.

constitutive law to generate the momentum over the entire geodesic. This momentum is used to generate the vector field and integrating the diffeomorphism. Shown in panel 4 is the density α showing the concentration near the boundary of I_0 . Shown in panel 5 are a comparison of the predicted directions of the momentum based on the gradient ∇I_0 compared to LV_0 . Notice in almost all case the arrow and the straight line superimpose as one line indicating the same direction. Panel 6 indicates that the vector field V_0 demonstrating that while α and the momentum LV_0 are highly localized, the velocity of motion extends over the entire object.

Shown in Figure 6 are similar results for the scale experiment.

Shown in Figure 7 are two sets of results for the geodesic shooting of the mitochondria. The organization of the results are the same as for the translation and scale experiments. Shown in Figure 7 are two sets of results for the geodesic shooting of the mitochondria. The organization of the results are the same as for the translation and scale experiments.

7. DISCUSSION

This paper focusses on the comparison of natural shapes in imagery using diffeomorphisms [5, 34, 9, 14, 21, 20] the natural extension of the finite dimensional matrix groups. Shapes and

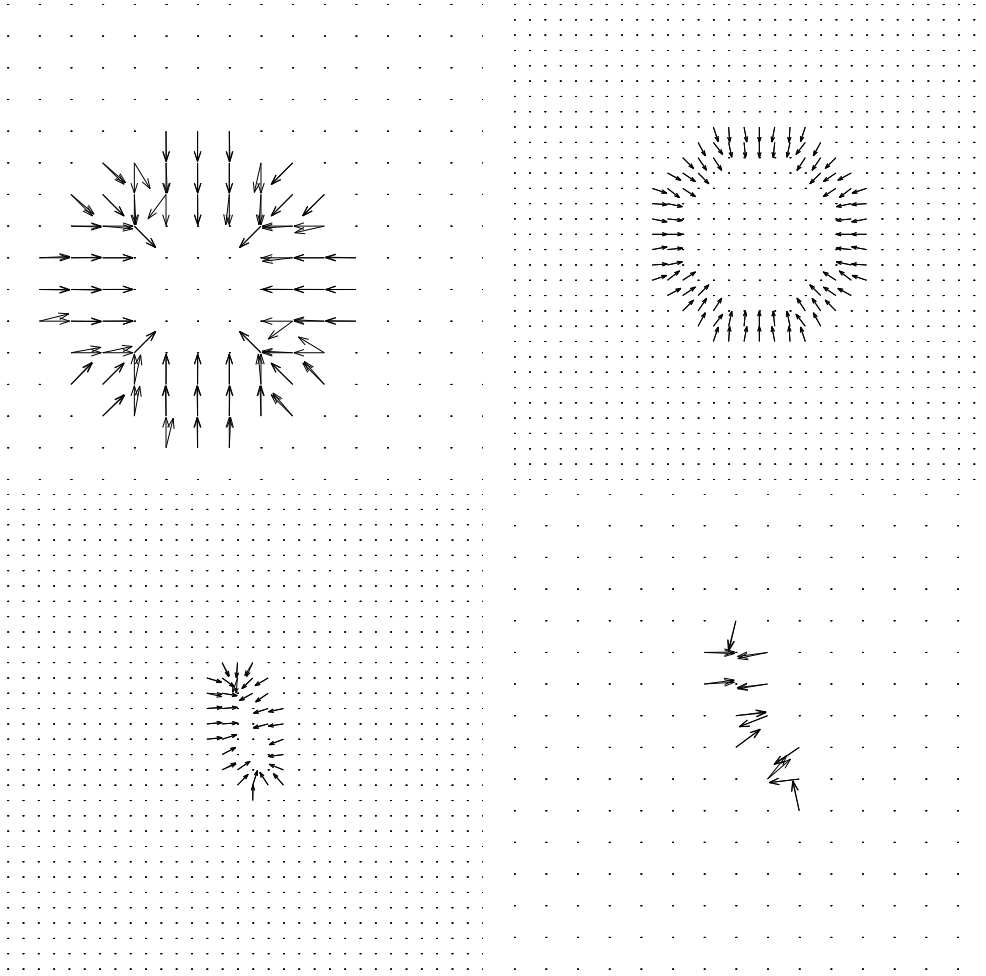


FIGURE 4. Figure shows comparison between momentum at the identity LV_0 and the gradient of the image ∇I_0 . Shown superimposed at every point in the grid are the arrow depicting the direction vector of each.

imagery are studied as an orbit via the action of diffeomorphic transformation. Diffeomorphisms $g \in \mathcal{G}$ defined on the background space $X \subset \mathbb{R}^d$ act on the shapes and images $I \in \mathcal{J}$ generating the orbit:

$$\mathcal{J} = \mathcal{G} \cdot I = \{I = I_\alpha \circ g, g \in \mathcal{G}\}. \quad (41)$$

The anatomical orbit or deformable template is made into a metric space with a metric distance between elements by constructing curves through the space of diffeomorphisms connecting them; for each $g, h \in \mathcal{G}$, then $g_t, t \in [0, 1]$ is constructed connecting the diffeomorphisms according to the flow $\frac{d\phi_t}{dt} = v_t \circ \phi_t$, $\phi_0 = g$, $\phi_1 = h$, $t \in [0, 1]$. This is the principal focus in Computational Anatomy, the study of shape via high dimensional transformation generated via the flows of Eqn.

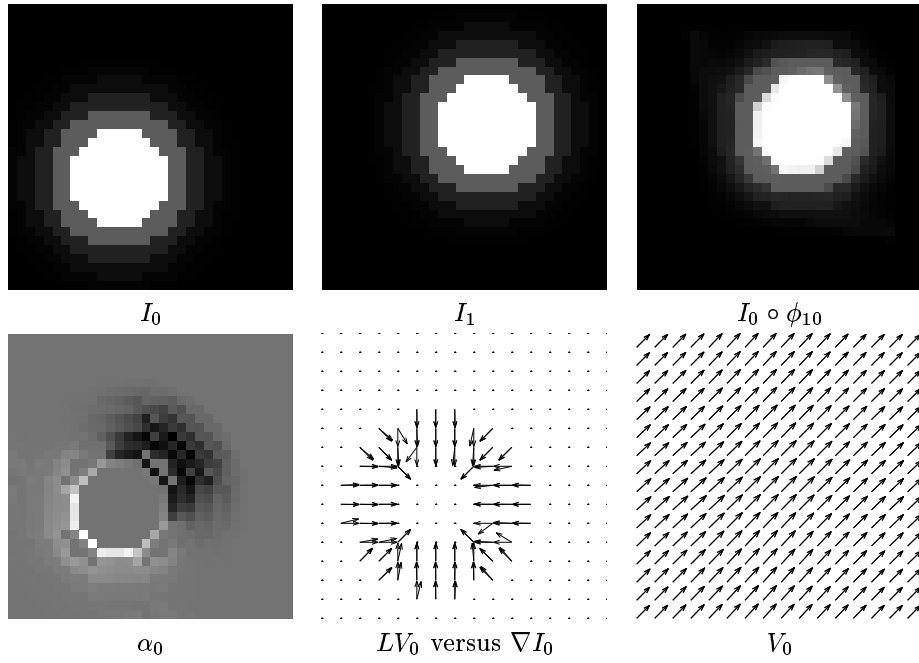


FIGURE 5. Rows 1,2: Results from translation experiment. Panels 1,2, and 3 show I_0 , I_1 , $I_0 \circ \phi_{10}$. Panel 4,5 and 6 show α_0 , LV_0 versus ∇I_0 , and V_0 and $L^{-1}\alpha\nabla I_0$. Rows 3,4: Results from scale experiment.

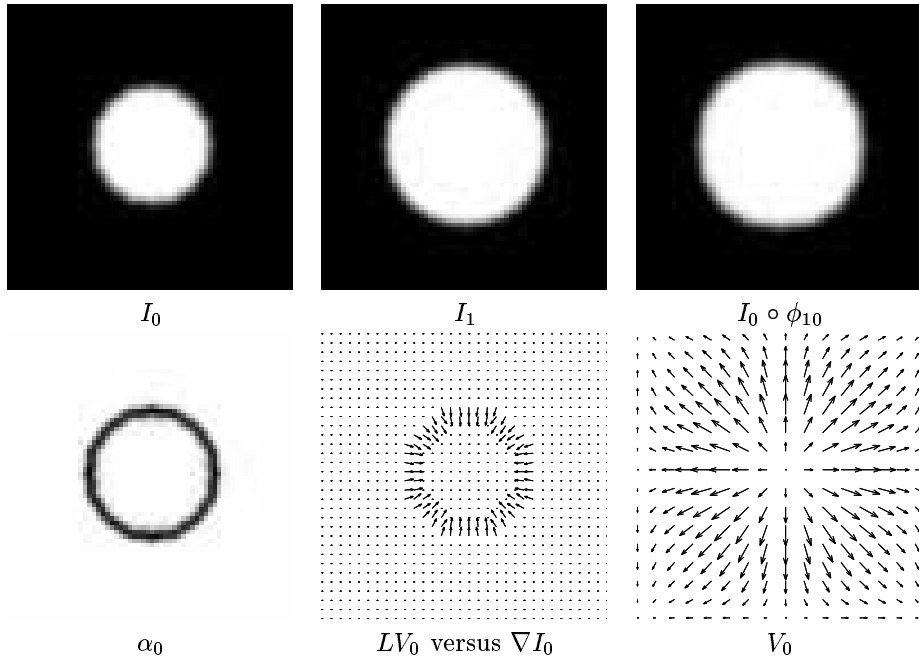


FIGURE 6. Rows 1,2: Results from scale experiment. Panels 1,2, and 3 show I_0 , I_1 , $I_0 \circ \phi_{10}$. Panel 4,5 and 6 show α_0 , LV_0 versus ∇I_0 , and V_0 and $L^{-1}\alpha\nabla I_0$.

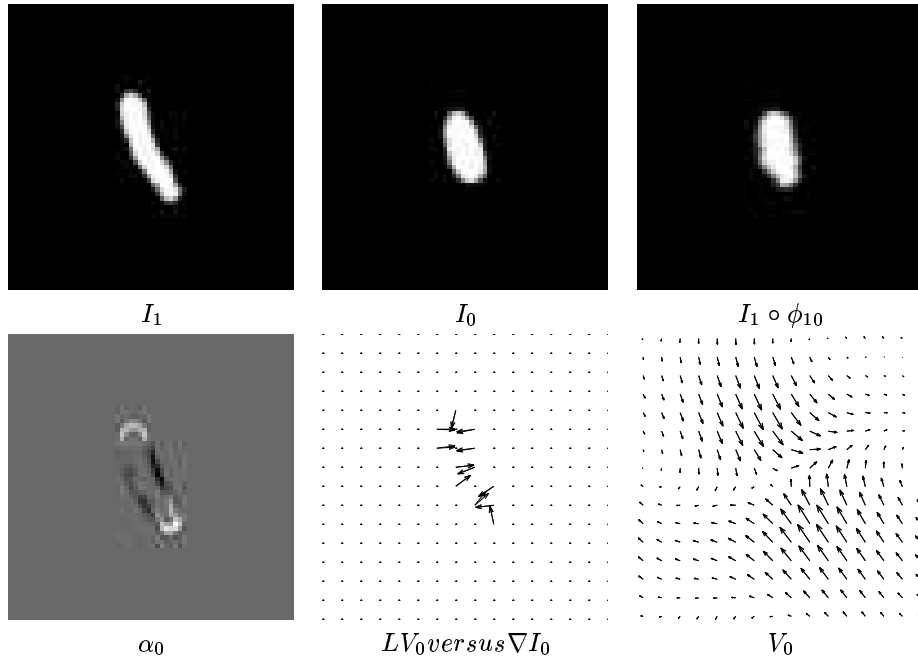


FIGURE 7. Results from mitochondria 2. Panels 1,2, and 3 show I_1 , I_0 , $I_1 \circ \phi_{10}$. Panel 4,5 and 6 show α_0 , LV_0 versus ∇I_0 , and V_0 .

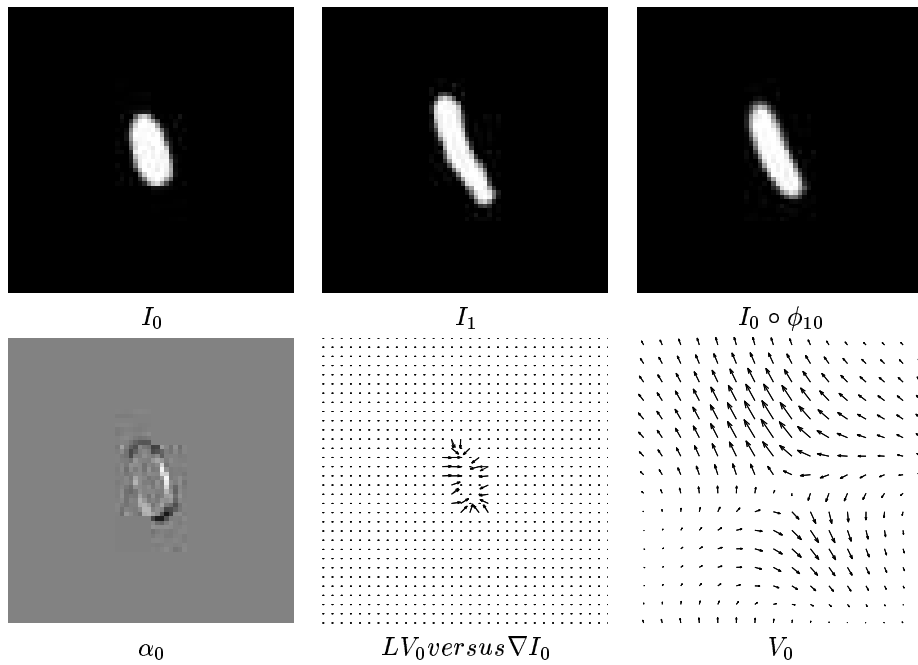


FIGURE 8. Results from mitochondria 1. Panels 1,2, and 3 show I_0 , I_1 , $I_0 \circ \phi_{10}$. Panels 4,5 and 6 show α_0 , LV_0 versus ∇I_0 , and V_0 .

1. To construct the metric the length of the curves connecting the group elements is defined according to $\text{Length}(g_t, t \in [0, 1]) = \int_0^1 \|v_t\|_V dt$, where the vector fields $v_t \in V$ the Hilbert

space with norm $(V, \|\cdot\|_V)$. The metric is defined according to $\|\cdot\|_V = \langle L\cdot, \cdot \rangle_2$, with L a mixture of differential operators; essentially V is a Sobolev space, with finiteness of the norm implying sufficient differentiability (smoothness) ensuring that the ODE integrates and is a flow of diffeomorphisms. The Riemannian metric in the group becomes the infimum over all curves connecting the group elements. This gives rise to a natural variational problem describing the geodesic flows between elements in the orbit, with the solution of the associated Euler-Lagrange equations giving the optimal flow of diffeomorphisms and thus the metric between the shapes. The metric on the orbit is then naturally extended to the orbit \mathcal{J} through the metric on the diffeomorphisms.

This paper examines the generation of the geodesics associated with the metric from several points of view, the first the Euler equation describing the geodesic diffeomorphic flow, and the second the variational formulation of the geodesic in terms of the minimizing flow of vector fields which generate them. The first formulation provides the connection of the Euler equation as the natural generalization of the classical work of geodesics in the finite dimensional Lie group to the infinite dimensional case. As well, it provides the link to Arnold's work on the subgroup of volume preserving diffeomorphisms corresponding to the divergence free case.

As we have shown, changing our point of view to the vector fields links us to the notions of geodesic evolution of the momentum. It is the momentum which is naturally normal to the level sets, not the vector fields themselves. There is no consistent (diffeomorphic flow) motion which has the vector fields themselves evolution normally. This is simply a result of the fact that we have shown that there do not exist solutions to the variational problem in the space of diffeomorphisms associated with momentum with $L = \text{identity}$.

This of course links our work on geodesics to the rapidly growing community working in *level set methods*. Interestingly, as we have shown, it is not the vector fields $v_t, t \in [0, 1]$ which are normal associated with geodesic motion, but rather it is the momentum $Lv_t, t \in [0, 1]$. The relation to level set methods is that in such approaches vector fields are defined which give the boundary manifold of the shape some normal velocity of motion, As we have shown, the *normal geodesic*

motion $Lv_t, t \in [0, 1]$ corresponds the velocity of motion $v_t, t \in [0, 1]$ of the shape being supported over the entire background space, thereby giving the global property that the resulting integrated vector field generates a diffeomorphism on the entire extrinsic space. This in turn carries the smooth submanifold diffeomorphically.

REFERENCES

- [1] I. Arnold, V. *Mathematical Methods of Classical Mechanics*. Springer, 1989. First Edition 1978.
- [2] V. Arnold and B. Khesin. Topological methods in hydrodynamics. *Ann. Rev. Fluid Mech.*, 24:145–166, 1992.
- [3] V. I. Arnold. Sur la géométrie différentielle des groupes de Lie de dimension infinie et ses applications à l'hydrodynamique des fluides parfaits. *Ann. Inst. Fourier (Grenoble)*, 1:319–361, 1966.
- [4] T. Chen and D. Metaxas. Image segmentation based on the integration of markov random fields and deformable models. In *Medical Image Computing and Computer-Assisted Intervention - Miccai 2000*, volume 1935 of *Lecture Notes in Computer Science*, pages 256–265. Springer-Verlag, 2000.
- [5] G. E. Christensen, R. D. Rabbitt, and M. I. Miller. Deformable templates using large deformation kinematics. *IEEE Trans. Image Processing*, 5(10):1435–1447, October 1996.
- [6] I. Cohen, L. Cohen, and N. Ayache. Using deformable surfaces to segment 3-d images and infer differential structures. *Computer Vision Graphics Image Processing*, 56(2):242–263, 1992.
- [7] T. Cootes, C. Taylor, D. Cooper, and J. Graham. Active shape models—their training and application. *Comp. Vision and Image Understanding*, 61(1):38–59, 1995.
- [8] C. Delfour, M and J.-P. Zolésio. *Shapes and Geometries. Analysis, differential calculus and optimization*. SIAM, 2001.
- [9] P. Dupuis, U. Grenander, and M. Miller. Variational problems on flows of diffeomorphisms for image matching. *Quart. App. Math.*, 56:587–600, September 1998.
- [10] A. Garrido and N. P. De la Blanca. Physically-based active shape models: Initialization and optimization. *Pattern Recognition*, 31(8):1003–1017, 1998.
- [11] U. Grenander. *General Pattern Theory*. Oxford Univ. Press, 1994.
- [12] U. Grenander, Y. Chow, and D. Keenan. *HANDS: A Pattern Theoretic Study of Biological Shapes*. Springer-Verlag, New York, 1990.
- [13] U. Grenander and M. I. Miller. Representations of knowledge in complex systems. *J. Roy. Stat. Soc. B*, 56(3):549–603, 1994.
- [14] U. Grenander and M. I. Miller. Computational anatomy: An emerging discipline. *Quart. App. Math.*, 56:617–694, 1998.
- [15] S. Joshi and M. I. Miller. Landmark matching via large deformation diffeomorphisms. *IEEE Trans. Image Processing*, 9(8):1357–1370, August 2000.
- [16] M. Kass, A. Witkin, and D. Terzopolous. Snakes: Active contour models. *International Journal of Computer Vision*, 1(4):321–331, 1988.
- [17] E. Marsden, J and S. Ratiu, T. *Introduction to Mechanics and Symmetry*. Springer, 1994.
- [18] M. Mignotte and J. Meunier. A multiscale optimization approach for the dynamic contour- based boundary detection issue. *Computerized Medical Imaging and Graphics*, 25(3):265–275, 2001.
- [19] M. Miller, S. Joshi, D. R. Maffitt, J. G. McNally, and U. Grenander. Mitochondria, membranes and amoebae: 1,2 and 3 dimensional shape models. In K. Mardia, editor, *Statistics and Imaging*, volume II. Carfax Publishing, Abingdon, Oxon., 1994.
- [20] M. Miller, A. Trouvé, and L. Younes. On the metrics and Euler-Lagrange equations of computational anatomy. *Annual Review of Biomedical Engineering*, 4:375–405, 2002.
- [21] M. Miller and L. Younes. Group actions, homeomorphisms, and matching: A general framework. *International Journal of Computer Vision*, 41(1/2):61–84, 2001.
- [22] J. Montagnat and H. Delingette. Volumetric medical images segmentation using shape constrained deformable models. In *Cormed-Mrcas'97*, volume 1205 of *Lecture Notes in Computer Science*, pages 13–22. Springer-Verlag, 1997.
- [23] J. Montagnat, H. Delingette, and N. Ayache. A review of deformable surfaces: topology, geometry and deformation. *Image and Vision Computing*, 19(14):1023–1040, 2001.
- [24] D. Mumford. Pattern theory and vision. In *Questions Mathématiques En Traitement Du Signal et de L'Image*, chapter 3, pages 7–13. Institut Henri Poincaré, 1998.
- [25] S. Osher and A. Sethian, J. Front propagating with curvature dependent speeds: algorithms based on hamilton-jacobi formulation. *Journal of Comp. Physics*, 79:12–49, 1988.
- [26] D. Pham, C. Xu, and J. Prince. Current methods in medical image segmentation. *Ann. Rev. Biomed. Engng.*, 2:315–337, 2000.
- [27] N. Schultz and K. Conradsen. 2d vector-cycle deformable templates. *Signal Processing*, 71(2):141–153, 1998.

- [28] S. Sclaroff and L. F. Liu. Deformable shape detection and description via model-based region grouping. *Ieee Transactions on Pattern Analysis and Machine Intelligence*, 23(5):475–489, 2001.
- [29] L. Staib and J. Duncan. Boundary finding with parametrically deformable models. *IEEE Trans. Pattern Analysis and Machine Intelligence*, 14:1061–1075, 1992.
- [30] L. Staib and J. Duncan. Model-based deformable surface finding for medical images. *IEEE Trans. Medical Imaging*, 15(5):1–13, October 1996.
- [31] D. Terzopoulos and D. Metaxas. Dynamic models with local and global deformations: Deformable superquadrics. *IEEE Trans. Patt. Anal. Mach. Intell.*, 13:703–714, 1991.
- [32] A. Trouvé and L. Younes. Local analysis on a shape manifold. Technical report, Université Paris 13, 2002.
- [33] A. Trouvé. Action de groupe de dimension infinie et reconnaissance de formes. C. R. Acad. Sci. Paris, Série I, (321):1031–1034, 1995.
- [34] A. Trouvé. Diffeomorphisms groups and pattern matching in image analysis. *Int. J. Computer Vision*, 28:213–221, 1998.
- [35] M. Vaillant and C. Davatzikos. Finding parametric representations of the cortical sulci using an active contour model. *Medical Image Analysis*, 1(4):295–315, 1997.
- [36] C. F. Westin, L. M. Lorigo, O. Faugeras, W. E. L. Grimson, S. Dawson, A. Norbash, and R. Kikinis. Segmentation by adaptive geodesic active contours. In *Medical Image Computing and Computer-Assisted Intervention - Miccai 2000*, volume 1935 of *Lecture Notes in Computer Science*, pages 266–275. Springer-Verlag, 2000.
- [37] C. Xu, D. L. Pham, and J. L. Prince. Finding the brain cortex using fuzzy segmentation, isosurfaces and deformable surface models. In *XVth Int. Conf on info Proc in Medicl Imaging*, June 1997.
- [38] C. Xu, D. L. Pham, and J. L. Prince. Medical image segmentation using deformable models. In J. Fitzpatrick and M. Sonka, editors, *SPIE Handbook on Medical Imaging – Volume III: Medical Image Analysis*, pages 129–174. SPIE, Bellingham, WA, 2000.
- [39] C. Xu and J. L. Prince. Gradient vector flow: A new external force for snakes. *CVRP*, Nov. 1997.
- [40] C. Xu and J. L. Prince. Gradient vector flow deformable models. In I. Bankman, editor, *Handbook of Medical Imaging*. Academic Press, San Diego, CA, 2000.
- [41] A. Yezzi, A. Tsai, and A. Willsky. A fully global approach to image segmentation via coupled curve evolution equations. *Journal of Visual Communication and Image Representation*, 13(1-2):195–216, 2002.
- [42] E. Zeidler. *Applied Functional Analysis. Applications to mathematical physics*. Springer, 1995.

CENTER OF IMAGING SCIENCE & DEPARTEMENT OF BIOMEDICAL ENGINEERING, THE JOHN HOPKINS UNIVERSITY, 301 CLARK HALL, BALTIMORE, MD 21218
E-mail address, M. I. Miller: mim@cis.jhu.edu

LABORATOIRE ANALYSE GÉOMÉTRIE ET APPLICATIONS & LABORATOIRE DE TRAITEMENT ET TRANSPORT DE L'INFORMATION, INSTITUT GALILÉE, UNIVERSITÉ PARIS 13, 93430 VILLETANAUSE, FRANCE
E-mail address, A. Trouvé: trouve@math.univ-paris13.fr

ECOLE NORMALE SUPÉRIEURE DE CACHAN, 61 AV. PRÉSIDENT WILSON, F-94235 CACHAN CEDEX, FRANCE
E-mail address, L. Younes: Laurent.Younes@cmla.ens-cachan.fr